

A light CP-odd Higgs boson and the muon anomalous magnetic moment

John F. Gunion

Department of Physics, University of California, Davis, CA 95616

ABSTRACT: We amalgamate the many experimental limits on the $abb\bar{b}$ coupling of a light CP-odd Higgs boson, a , including model-dependence coming from the ratio of the $at\bar{t}$ to the $abb\bar{b}$ coupling. We then employ these limits to analyze the extent to which a light a can make a significant contribution to the discrepancy, Δa_μ , between the experimentally observed a_μ and that predicted by the standard model. In a “model-independent” framework and in the context of a general two-Higgs-doublet model this is a significant possibility. In contrast, the minimal supersymmetric model is too strongly constrained (after combining experimental and theoretical input) to allow a CP-odd- a explanation of Δa_μ . The next-to-minimal supersymmetric model allows more freedom and the light a of the model could explain the full Δa_μ if $9.2 \text{ GeV} < m_a < 12 \text{ GeV}$, or contribute substantially for larger m_a , if $\tan \beta$ is large.

There have been numerous studies [1, 2, 3, 4, 5, 6, 7, 8, 9, 10, 11, 12] of the extent to which the Higgs sector could contribute to the anomalous magnetic moment of the muon, a_μ , with current focus on whether it could be used to explain some portion of the now $\sim 3\sigma$ positive deviation of a_μ with respect to the Standard Model (SM) prediction. The numerical deviation is variously quoted as $\Delta a_\mu \sim (27.5 \pm 8.4) \times 10^{-10}$ [13] or $(27.7 \pm 9.3) \times 10^{-10}$ [12]. It is becoming increasingly likely that this deviation can only be explained by new physics of some kind and a beyond-the-standard-model Higgs sector has always been a prime candidate.

Precision electroweak data and direct LEP limits on a light CP-even scalar suggest that it should have SM-like couplings and substantial mass, in which case its contribution to a_μ will only be of order $few \times 10^{-11}$. Thus, we will focus on the possible contribution, δa_μ , of a light CP-odd Higgs boson, a , of a CP-conserving Higgs sector, for which it is critical [1] to include the two-loop Barr-Zee type diagrams [14] since the one-loop a_μ contribution is negative whereas the two-loop contribution is positive in popular models.

Of particular interest is the $m_a < 2m_b$ region, for which a light Higgs, h , with SM-like WW , ZZ and fermionic couplings can have mass $m_h \sim 100$ GeV while still being consistent with LEP data by virtue of $h \rightarrow aa \rightarrow 4\tau$ decays being dominant [15, 16, 17, 18] (see also [19, 20]). Such a Higgs provides perfect agreement with the rather compelling precision electroweak constraints, and for $BR(h \rightarrow aa) \gtrsim 0.75$ also provides an explanation for the $\sim 2.3\sigma$ excess observed at LEP in $e^+e^- \rightarrow Zb\bar{b}$ in the region $M_{b\bar{b}} \sim 100$ GeV. We term this the “ideal” Higgs scenario. More generally, we will only consider models for which the ZZh coupling is SM-like (implying zero Zha coupling and therefore no lower limits on m_a coming from $e^+e^- \rightarrow ha$ at LEP) and m_h is such as to give good agreement with precision electroweak data.

Possible contributions to a_μ by the a depend crucially on the $a\mu^-\mu^+$, $ab\bar{b}$ and $at\bar{t}$ couplings defined via

$$\mathcal{L}_{af\bar{f}} \equiv iC_{af\bar{f}} \frac{ig_2 m_f \bar{f}}{2m_W} \gamma_5 f a. \quad (1)$$

We assume a Higgs model in which $C_{a\mu^-\mu^+} = C_{a\tau^-\tau^+} = C_{ab\bar{b}}$, as typified by a two-Higgs-doublet model (2HDM) of either type-I or type-II (a 2HDM contains Higgs bosons h, H with $m_H > m_h$, a and h^+), or more generally if the lepton and quark masses are generated by the same combination of Higgs fields. (Much larger values of a_μ relative to those we find below are possible in models in which $r = (C_{a\mu^-\mu^+} = C_{a\tau^-\tau^+})/C_{ab\bar{b}} \gg 1$ — such models include those in which the muon and tau masses are generated by different Higgs fields than the b mass. For $r \neq 1$, our results for δa_μ should be rescaled by r .) In a 2HDM of type-II and in the MSSM, $C_{a\mu^-\mu^+} = C_{ab\bar{b}} = \tan \beta$ (where $\tan \beta = h_u/h_d$ is the ratio of the vacuum expectation values for the doublets giving mass to up-type quarks vs. down-type quarks) and $C_{at\bar{t}} = \cot \beta$. In the NMSSM the expressions for $C_{a\mu^-\mu^+} = C_{ab\bar{b}}$ and $C_{at\bar{t}}$ include an additional factor discussed later. In a type-I 2HDM, $C_{a\mu^-\mu^+} = C_{a\tau^-\tau^+} = C_{ab\bar{b}} = -C_{at\bar{t}} = -\cot \beta$. In the most general Higgs model, $C_{a\mu^-\mu^+}$, $C_{a\tau^-\tau^+}$, $C_{ab\bar{b}}$ and $C_{at\bar{t}}$ will be more complicated functions of the vevs of the Higgs fields and the structure of the Yukawa couplings. In this paper, we assume $C_{a\mu^-\mu^+} = C_{a\tau^-\tau^+} = C_{ab\bar{b}}$ but allow for general values of $R_{b/t}^2 \equiv C_{ab\bar{b}}/C_{at\bar{t}}$. We consider only positive values of $R_{b/t}^2$

since only these are of relevance for explaining the observed positive Δa_μ and positive values are typical of most models.

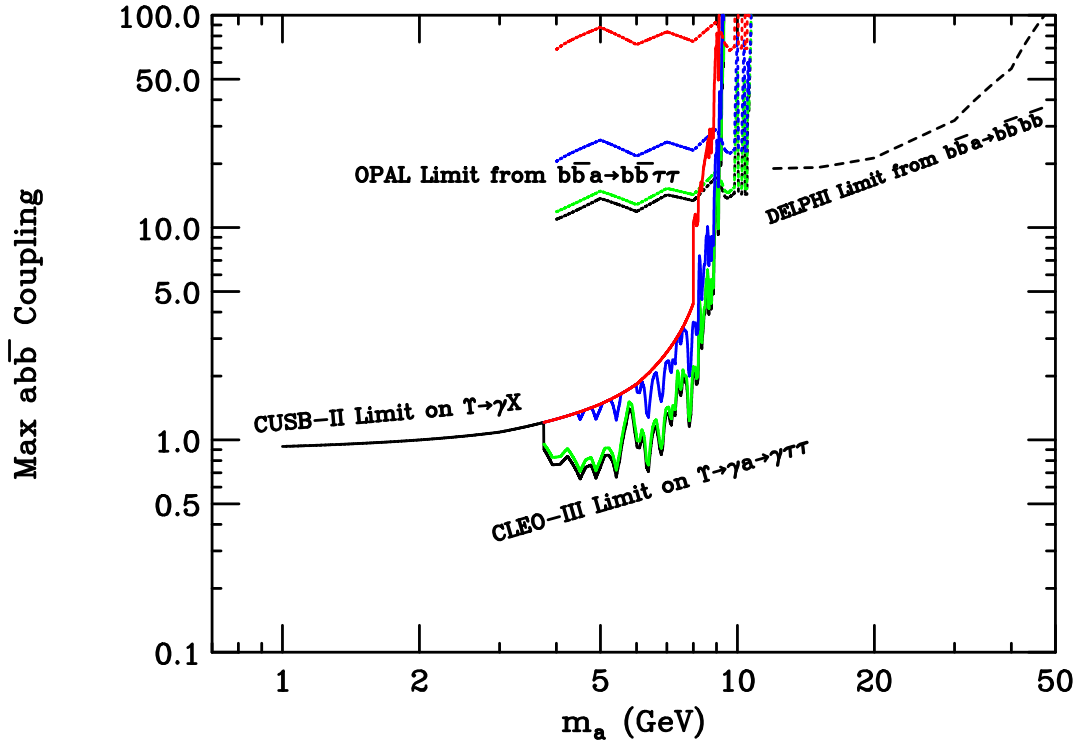


Figure 1: Upper limit, $C_{ab\bar{b}}^{\max}$, on $|C_{ab\bar{b}}|$ as a function of m_a coming directly from experimental data. In the case of limits based on $a \rightarrow \tau^+\tau^-$, curves for $R_{b/t} = 0.5$ (red), 1 (blue), 2 (green), 10 (black) are shown with $R_{b/t} = 10$ giving the lowest curves and $R_{b/t} = 0.5$ giving the highest curves.

Limits on $|C_{ab\bar{b}}|$ come from $\Upsilon \rightarrow \gamma a$ decays at B factories and $e^+e^- \rightarrow b\bar{b}a$ production at LEP. For $m_a < 2m_\tau$ the strongest limits come from the old (90% CL – all other limits employed here are 95% CL) CUSB-II limits [21] on $BR(\Upsilon \rightarrow \gamma X)$, where X is assumed to be visible. For $2m_\tau < m_a < 9.2$ GeV, the recent CLEO-III [22] limits on $\Upsilon \rightarrow \gamma a \rightarrow \gamma\tau\tau$ are the strongest (in interpreting these limits one must account for the value of $BR(a \rightarrow \tau^+\tau^-)$ — this in turn depends on $R_{b/t}$, but very weakly for $R_{b/t} \geq 2$, see below). For 9.2 GeV $< m_a < m_\Upsilon$, mixing of the a with various η_b and χ_0 bound states becomes crucial [23]. Ref. [22] gives results for $C_{ab\bar{b}}^{\max}$ in this m_a range without taking this mixing into account but notes that their limits cannot be relied upon for $m_a > 9.2$ GeV. Whether additional limits can be extracted from lepton non-universality studies in the $9.2 < m_a < m_\Upsilon$ region is being studied [24]. OPAL limits [25] (which assume $BR(a \rightarrow \tau^+\tau^-) = 1$) on $e^+e^- \rightarrow b\bar{b}\tau\tau$ become numerically relevant for roughly 9 GeV $< m_a < 2m_b$. Ref. [25] converts these limits to limits on the $ab\bar{b}$ coupling using the modeling of [23]. These are the only limits in the $m_\Upsilon < m_a < 2m_b$ range and continue to be relevant up to 12 GeV. Above $m_a = 2m_b$ these $ab\bar{b}$ coupling limits become quite weak due to the $\eta_b - a$ mixing and the decrease of $BR(a \rightarrow \tau\tau)$. For $m_a \geq 12$ GeV, limits on the $ab\bar{b}$ coupling can be extracted from

$e^+e^- \rightarrow b\bar{b}a \rightarrow b\bar{b}b\bar{b}$ [26]. The maximum value of $|C_{abb}|$ allowed by all these various limits, C_{abb}^{\max} , is shown in Fig. 1 as a function of m_a for several values of $R_{b/t}$ ($R_{b/t} = 0.5, 1, 2, 10$). Note that there is almost no dependence of C_{abb}^{\max} on $R_{b/t}$ for $R_{b/t} \geq 2$. Values of $|C_{abb}|$ above 50 raise issues of non-perturbativity of the abb coupling and are likely to be in conflict with Tevatron limits on $b\bar{b}a$ production [27]. C_{abb}^{\max} depends on $R_{b/t}$ when the CLEO-III $\Upsilon \rightarrow \gamma a \rightarrow \gamma\tau^+\tau^-$ or OPAL $b\bar{b}a \rightarrow b\bar{b}\tau^+\tau^-$ limits are the most relevant. What is new in this paper is the systematic incorporation of the $R_{b/t}$ dependence of C_{abb}^{\max} and the systematic incorporation of the C_{abb}^{\max} limits in the context of predictions for δa_μ in a wide class of models.

In the case of the simple 2HDM(II), where $C_{abb} = R_{b/t} = \tan\beta$, values of m_a for which $\tan\beta > C_{abb}^{\max}(\tan\beta)$ are not allowed in the model context. These disallowed regions typically emerge in the range $m_a < 8$ GeV for $\tan\beta = 1$ rising to $m_a \lesssim 10$ GeV for higher $\tan\beta$; at higher $\tan\beta$ values they have a complicated structure that we will discuss later. In addition, a disallowed region also arises over a limited m_a range starting from $m_a > 12$ GeV when $\tan\beta \gtrsim 18$, the larger the value of $\tan\beta$ the larger the interval. For example, for $\tan\beta = 50$ the DELPHI limits imply that the 2HDM(II) is not consistent for $12 \lesssim m_a \lesssim 37$ GeV and the OPAL and Upsilon limits imply that the 2HDM(II) is not consistent for $m_a < 10$ GeV. In contrast, for $\tan\beta = 10$ the 2HDM(II) model is always consistent with the DELPHI limits and is only inconsistent (with CLEO-III and CUSB limits) for $m_a \lesssim 9$ GeV. These 2HDM(II) results are an update of the results obtained in [8]. The results in all other models, in particular in the NMSSM context are new.¹

We will now explore the implications for a_μ . Since the two-loop contributions include that with a t -loop as well as those with b and τ loops, we must specify the value of C_{att} relative to C_{abb} in order to compute the contribution of a to a_μ for a given C_{abb} value. In a 2HDM of type-II, including the MSSM and NMSSM, $C_{att} = \cot\beta$ and after including the two-loop diagrams $\delta a_\mu > 0$ for $m_a > 2.6, 2, 0$ GeV if $\tan\beta > 5, 3, 1$. In a type-I 2HDM, $C_{att} = -C_{abb} = \cot\beta$. Then, the (dominant) top-loop Barr-Zee type diagram gives a negative contribution to a_μ and δa_μ is negative for all m_a . Only models with positive $R_{b/t}^2$ are of relevance for explaining the observed positive Δa_μ . Results for δa_μ employing the $C_{abb} = C_{abb}^{\max}$ limits as a function of m_a and $R_{b/t}$ and taking $R_{b/t} = 1, 3, 10$ and 50 are plotted in Fig. 2. (For $R_{b/t} < 1$, simply multiply the $R_{b/t} = 1$ curve by $1/R_{b/t}^2$.)

To a good approximation, $R_{b/t} \geq 50$ is equivalent to dropping the two-loop diagram containing the top quark and gives the smallest result. Since (for positive C_{abb}/C_{att}) the two-loop top diagram enters with the same (positive) sign as the b and τ two-loop diagrams, the largest δa_μ values are obtained for the smallest $R_{b/t}$ when using upper limits on the abb coupling as input. As a result, we see in Fig. 2 that for lower $R_{b/t}$ values ($1 < R_{b/t} \lesssim 3$) any value of $m_a \gtrsim 9$ GeV would make it possible to obtain $\delta a_\mu = \Delta a_\mu \sim 27.5 \times 10^{-10}$ for some choice of $C_{abb} \leq C_{abb}^{\max}$. For $R_{b/t} < 0.2$, for which C_{att} enters non-perturbative territory, $\delta a_\mu > \Delta a_\mu$ if $C_{abb} = C_{abb}^{\max}$ for all m_a so that agreement could always be obtained for some $C_{abb} < C_{abb}^{\max}$. However, for $R_{b/t} \gtrsim 10$ the full discrepancy can only be explained if $10 \text{ GeV} < m_a < 12 \text{ GeV}$ or $m_a \gtrsim 36 \text{ GeV}$. Recall, however, that the value of C_{abb}^{\max}

¹Several months after arXiv submission of this paper, similar results for the NMSSM were obtained in [28].

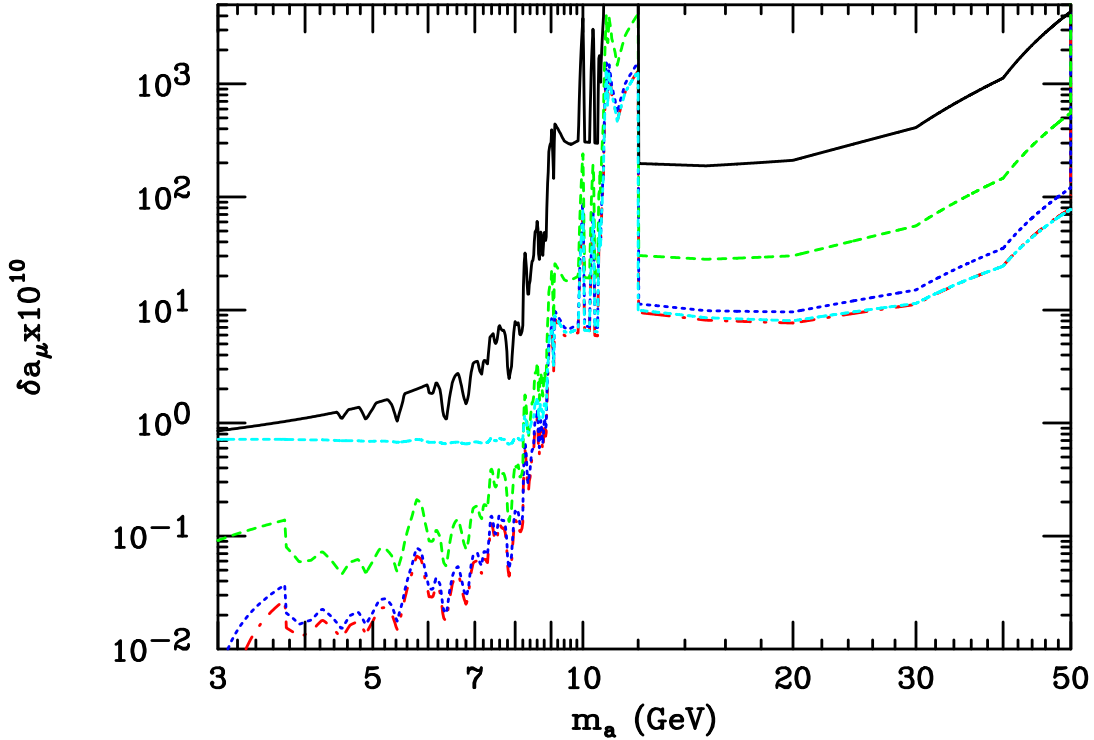


Figure 2: The value of δa_μ from CP-odd a loops is plotted as a function of m_a for $R_{b/t} = 1$ (black, solid), $R_{b/t} = 3$ (green, dashes), $R_{b/t} = 10$ (blue, dots) and $R_{b/t} = 50$ (red, long dash, short dot, lowest curve), assuming maximal $ab\bar{b}$ coupling, $C_{ab\bar{b}}^{\max}$, from Fig. 1. Also shown as the dotdash cyan curve is the 2HDM(II) prediction for $\tan\beta = C_{ab\bar{b}}^{\max}(\tan\beta)$, i.e. the largest possible (self-consistent) choice of $\tan\beta$ within the 2HDM(II) context. For $m_a \gtrsim 9$ GeV this latter curve coincides with the $R_{b/t} = 50$ curve.

extracted from the data in the former region relies on the modeling for the $a - \eta_b$ mixing employed in the experimental analysis. Also, for $m_a > 36$ GeV and $R_{b/t} \geq 10$, $\delta a_\mu = \Delta a_\mu$ requires non-perturbative $C_{ab\bar{b}} > 50$ values.

Of course, it is interesting to know what value of $C_{ab\bar{b}} < C_{ab\bar{b}}^{\max}$ is needed in order to match the observed $\Delta a_\mu = 27.5 \times 10^{-10}$ for those m_a and $R_{b/t}$ values for which this is possible. The results for the general case in which $C_{ab\bar{b}}$ is not correlated with $R_{b/t}$ are plotted in Fig. 3. In general, for low values of $R_{b/t}$ (for which the top loop is a major contributor to δa_μ) rather modest values of $C_{ab\bar{b}}$ will reproduce the observed Δa_μ . As $R_{b/t}$ increases, the bottom loop diagrams must reproduce Δa_μ on their own and increasingly large values of $C_{ab\bar{b}}$ are required. As we shall see, one particularly interesting range of m_a for $R_{b/t} \geq 10$ is $9.9 \text{ GeV} \lesssim m_a \lesssim 12 \text{ GeV}$. In Fig. 3, we see that in this m_a range the observed $\Delta a_\mu = 27.5 \times 10^{-10}$ is matched for $C_{ab\bar{b}}$ in the range $28 \leq C_{ab\bar{b}} \leq 32$ for $R_{b/t} \geq 10$ when $9.9 \text{ GeV} \lesssim m_a \lesssim 12 \text{ GeV}$.

The above results are modified in the context of more restrictive models. Fig. 4 shows the results for δa_μ in the type-II 2HDM, in which $C_{ab\bar{b}} = R_{b/t} = \tan\beta$, obtained for various $\tan\beta$ values. In the type-II 2HDM, the value of δa_μ is determined once $\tan\beta$ and m_a

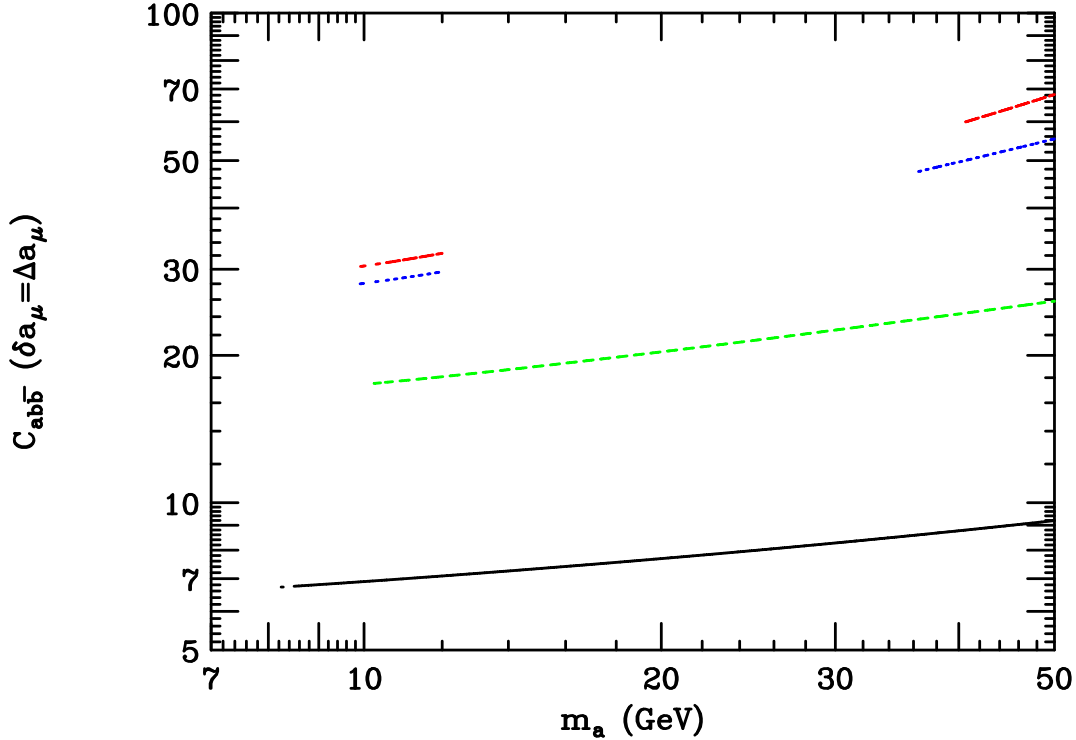


Figure 3: The value of $C_{ab\bar{b}}$ required in order that $\delta a_\mu = 27.5 \times 10^{-10}$ is plotted as a function of m_a for $R_{b/t} = 1$ (black, solid), $R_{b/t} = 3$ (green, dashes), $R_{b/t} = 10$ (blue, dots) and $R_{b/t} = 50$ (red, long dash, short dot, highest curve), for those choices of m_a such that the required $C_{ab\bar{b}}$ is less than $C_{ab\bar{b}}^{\max}$ as plotted in Fig. 1. Gaps for any given $R_{b/t}$ curve correspond to m_a values for which $C_{ab\bar{b}} > C_{ab\bar{b}}^{\max}$ would be required.

are specified. Unlike the very general case just considered, for which $R_{b/t}$ is not related to $C_{ab\bar{b}}$, in the 2HDM(II) context one cannot have large $C_{ab\bar{b}}$ without having large $R_{b/t}$, which then minimizes the very important (positive) top loop contribution. Thus, the largest δa_μ values are now obtained with large $\tan \beta$ values. The possibilities are also constrained by the requirement that $\tan \beta$ cannot exceed $C_{ab\bar{b}}^{\max}(\tan \beta)$. The gaps in the curves of Fig. 4 are those regions where $\tan \beta > C_{ab\bar{b}}^{\max}(\tan \beta)$. The result is that in order to obtain a value of δa_μ of order 27.5×10^{-10} that also has $\tan \beta \leq C_{ab\bar{b}}^{\max}(\tan \beta)$ requires a rather precisely fixed value of $\tan \beta \sim 30 - 32$ and $m_a \sim 9.9 - 12$ GeV (see the $\tan \beta = 32$ dotdash cyan curve). In the context of the most general CP-conserving type-II 2HDM, any value in the above small range is not excluded using combined Zh and ha LEP data [29] so long as $m_h \gtrsim 60$ GeV; and, there are no limits on m_a if $m_h \gtrsim 100$ GeV. Further, contributions to the precision electroweak observables S and T are tiny if $m_H = m_{h^+}$ when h has SM-like ZZh coupling. As a further remark, we note from trends as $\tan \beta$ increases apparent in Fig. 4 (lower plot) that for $\tan \beta$ values above 50 (i.e. outside the perturbative limit on this coupling) one will not be able to have $\tan \beta < C_{ab\bar{b}}^{\max}(\tan \beta)$ in the $m_a < 12$ GeV zone, but that at some largish value of m_a above about 40 GeV one *will* be able to achieve a

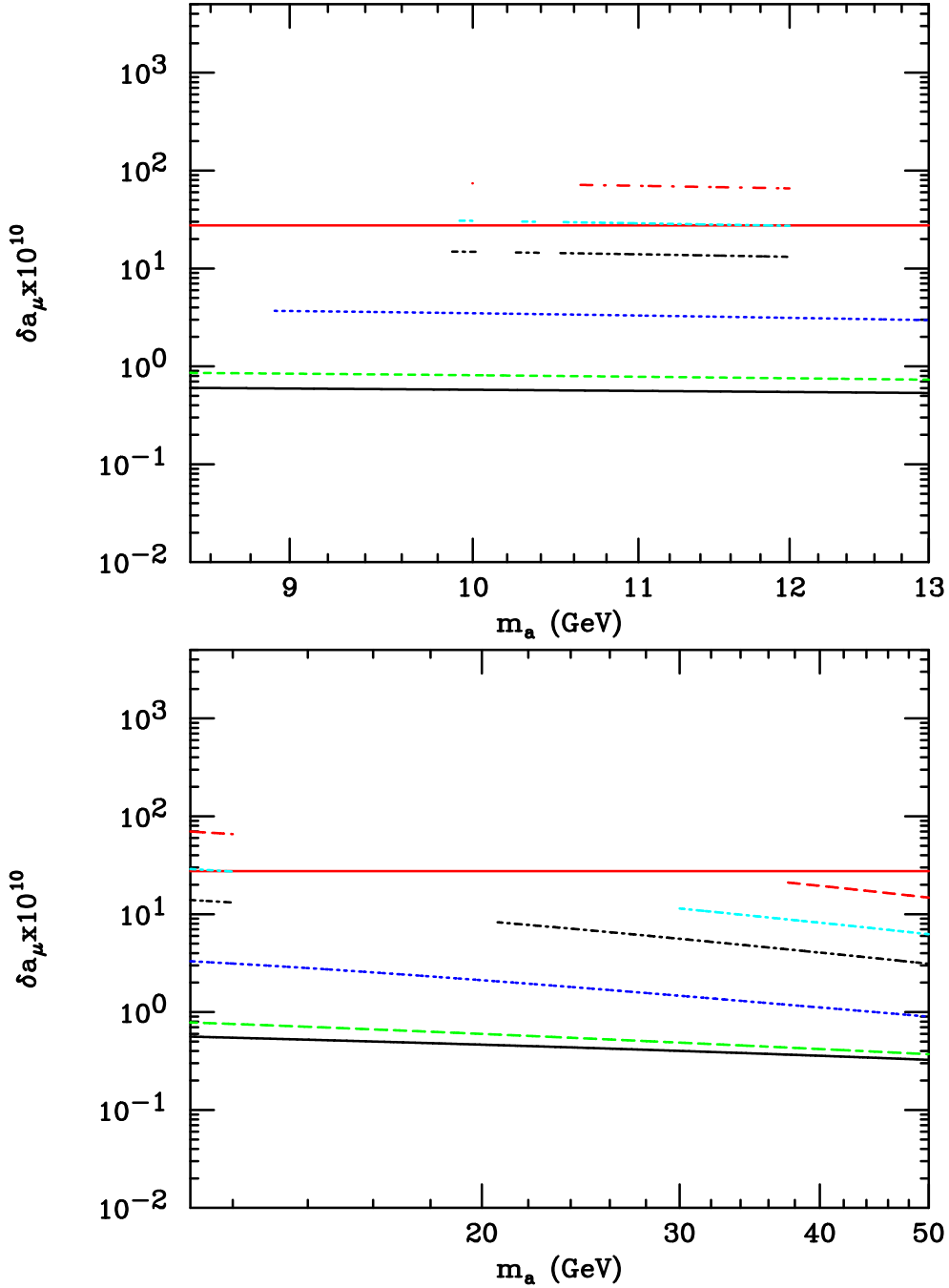


Figure 4: The value of δa_μ from CP-odd a loops is plotted as a function of m_a for $\tan\beta = 1$ (black, solid), $\tan\beta = 3$ (green, dashes), $\tan\beta = 10$ (blue, dots), $\tan\beta = 22$ (black, dotdash), $\tan\beta = 32$ (cyan, dotdash) and $\tan\beta = 50$ (red, long dash, short dot, highest curve), assuming the 2HDM(II) model with $R_{b/t} = \tan\beta$ and requiring that $\tan\beta \leq C_{abb}^{\max}(\tan\beta)$. Omitted regions are those for which $\tan\beta > C_{abb}^{\max}(\tan\beta)$ as plotted in Fig. 1. Note the multiple gaps for the $\tan\beta = 22, 32, 50$ cases in the $10 \text{ GeV} \leq m_a \leq 11 \text{ GeV}$ region. An intersection of the solid red line at $\delta a_\mu = 27.5 \times 10^{-10}$ with a 2HDM(II) curve essentially only occurs in the $\tan\beta = 32$ case.

match to Δa_μ . This is because the DELPHI limits on C_{abb} deteriorate so rapidly as m_a increases above 40 GeV.

As a further perspective on the 2HDM(II) results, we plot in Fig. 2 the largest possible value of δa_μ within the 2HDM(II) as a function of m_a (the dotdash cyan curve). This maximal value is obtained when $\tan \beta = C_{abb}^{\max}(\tan \beta)$ (i.e. for the largest self-consistent choice of $\tan \beta$ such that $C_{abb} = \tan \beta$). Again it is apparent that δa_μ can match (or exceed) 27.5×10^{-10} in the range $9.9 \lesssim m_a \lesssim 12$ GeV. And, to repeat, matching in this range is always achieved for $\tan \beta \sim 30 - 32$.

The ability to achieve $\delta a_\mu = \Delta a_\mu$ is much more constrained in the popular Minimal Supersymmetric Model (MSSM). In the MSSM, the LEP lower limit on m_a is of order 90 – 100 GeV, depending upon $\tan \beta$ and precise model inputs [30]. For $m_a > 90$ GeV, $\delta a_\mu = \Delta a_\mu$ is only achievable for $C_{abb} = \tan \beta$ well above the upper bound of 50 employed here. (Of course, if the MSSM sparticles are light, their contributions could yield the observed Δa_μ [31].)

The Next-to-Minimal Supersymmetric model (NMSSM) provides more fertile ground. The NMSSM is obtained by adding a singlet superfield \widehat{S} to the MSSM Higgs superfields \widehat{H}_u and \widehat{H}_d . Ref. [32] was the first to consider the NMSSM Higgs sector phenomenology in detail. The scalar component of \widehat{S} contains one CP-even and one CP-odd scalar field. The resulting Higgs sector thus contains three CP-even Higgs bosons ($h_{1,2,3}$) and two CP-odd Higgs bosons ($a_{1,2}$), all of which can have a singlet component. A convenient program for exploring the NMSSM Higgs sector is NMHDECAY [33, 34]. We will not consider contributions to a_μ from sparticles as recently studied in [11, 12].

The NMSSM is especially attractive in that it allows for the “ideal” Higgs sector described earlier with $m_{h_1} \sim 100$ GeV, consistent with LEP data if $m_{a_1} < 2m_b$ and $BR(h_1 \rightarrow a_1 a_1) > 0.75$. For $m_{a_1} > 2m_b$, one must have $m_{h_1} \gtrsim 110$ GeV to avoid LEP bounds. (But, for $110 \text{ GeV} \lesssim m_{h_1} \lesssim 163 \text{ GeV}$, so long as the ZZh_1 coupling is SM-like the agreement with precision electroweak data is still within the 95% CL limit unless only the “leptonic” determination of $\sin^2 \theta_\ell^{\text{eff}}$ is employed in the precision electroweak analysis; the latter yields a much higher CL for the overall fit and requires $m_{h_1} \lesssim 105$ GeV at 95% CL — see [35] for details).

The most crucial parameter for the NMSSM analysis is $\cos \theta_A$ defined by

$$a_1 = \cos \theta_A a_{MSSM} + \sin \theta_A a_S, \quad (2)$$

where a_{MSSM} is the CP-odd (doublet) scalar in the MSSM sector of the NMSSM and a_S is the additional CP-odd singlet scalar of the NMSSM. In terms of $\cos \theta_A$, $C_{a\mu^-\mu^+} = C_{abb} = \cos \theta_A \tan \beta$ and $C_{at\bar{t}} = \cos \theta_A \cot \beta$.

Before proceeding, we consider possible constraints from precision electroweak data. Since the light SM-like h_1 already gives good agreement, the rest of the Higgs sector should give a small contribution to S and T (assuming sparticle contributions are not substantial). One finds that if m_{a_1} is in the range considered and h_1 is SM-like, then it is typically the case that either h_2 or h_3 is mainly singlet, denoted h_S , and the other, denoted here as h_D , is mainly doublet. Further, the $Zh_S a_1$ coupling is very tiny while the $Zh_D a_1$ coupling is maximal and $m_{h^+} \sim m_{a_2} \sim m_{h_D}$. With these inputs, one finds that the extra contributions from the Higgs sector to S and T are very small and the excellent agreement with precision electroweak constraints coming from the h_1 is preserved.

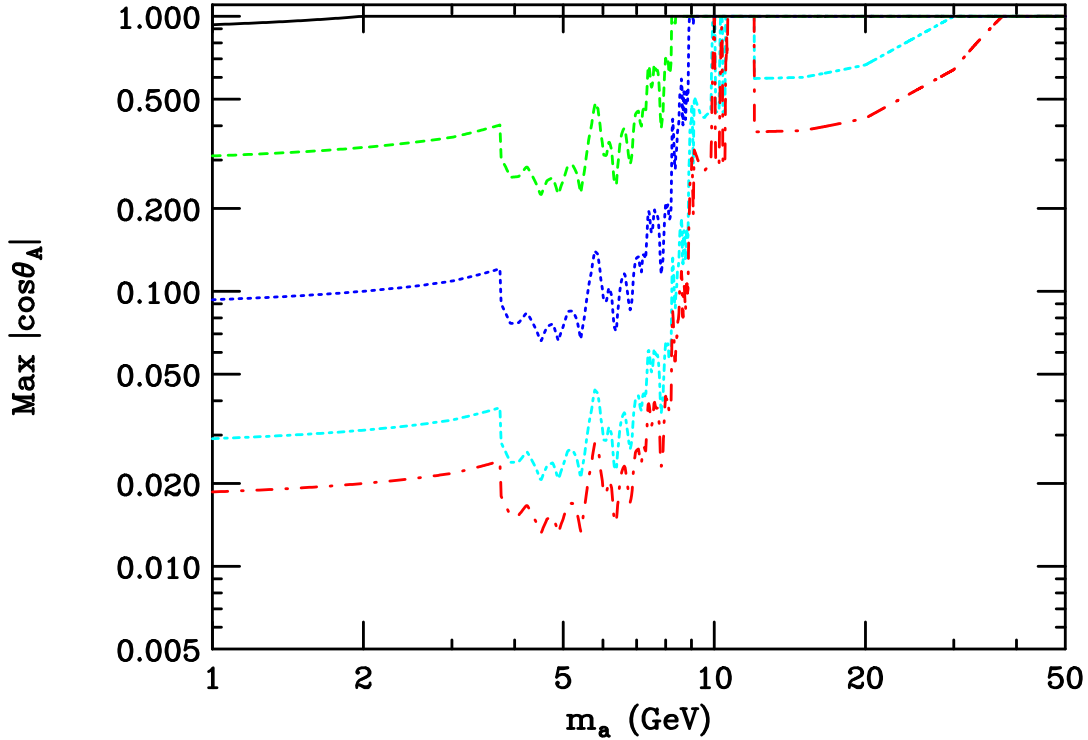


Figure 5: $\cos \theta_A^{\max}$ in the NMSSM (where $C_{ab\bar{b}} = \cos \theta_A \tan \beta$) as a function of m_a after requiring $\cos \theta_A^{\max} \tan \beta = C_{ab\bar{b}}^{\max}$ using the $C_{ab\bar{b}}^{\max}$ values of Fig. 1. The different curves correspond to $\tan \beta = 1$ (black, solid, upper curve), 3 (green, dashes), 10 (blue, dots), 32 (cyan, dotdash) and 50 (red, long dash, short dot, lowest curve).

Let us now consider $a_1 \equiv a$ contributions to a_μ for various fixed $\tan \beta$ values. Then, $\cos \theta_A$ is constrained by the requirement that $C_{ab\bar{b}} = \cos \theta_A \tan \beta \leq C_{ab\bar{b}}^{\max}$, which constrains $\cos \theta_A$ to very small values for low m_a and large $\tan \beta$. However, no matter what the value of $\tan \beta$, the extra freedom of adjusting $\cos \theta_A$ does allow us to avoid gaps in m_a for which $C_{ab\bar{b}} > C_{ab\bar{b}}^{\max}$. This, in turn, will give us more possibilities for δa_μ . Inputting the values of $C_{ab\bar{b}}^{\max}$ as a function of m_a we obtain the results of Fig. 5 for the maximum allowed value of $\cos \theta_A$ as a function of m_a for various $\tan \beta$ values.

We now turn to the resulting NMSSM predictions for a_μ . The value of δa_μ is largest for $\cos \theta_A = \cos \theta_A^{\max}$. The resulting values of δa_μ are plotted as a function of m_a in Fig. 6. As in the generic case, the strong constraints from Upsilon physics imply that significant contributions to a_μ are not possible until m_a exceeds roughly 9.2 GeV. To understand why δa_μ increases with increasing $\tan \beta$ for $m_a > 12$ GeV, whereas it decreases with increasing $\tan \beta$ for low m_a , we first note that the 2-loop, top-loop contribution to δa_μ is independent of $\tan \beta$ (because of a $C_{a\mu-\mu^+} + C_{at\bar{t}}$ structure that is $\tan \beta$ -independent), whereas the 2-loop bottom-loop contribution increases as $\tan^2 \beta$ (because of a $C_{a\mu-\mu^+} + C_{ab\bar{b}} \propto \tan^2 \beta$ structure). Numerically, before including the extra $\tan^2 \beta$ factor for the latter, the 2-loop, top-loop contribution is much larger than the 2-loop, bottom-loop contribution. Of course, both

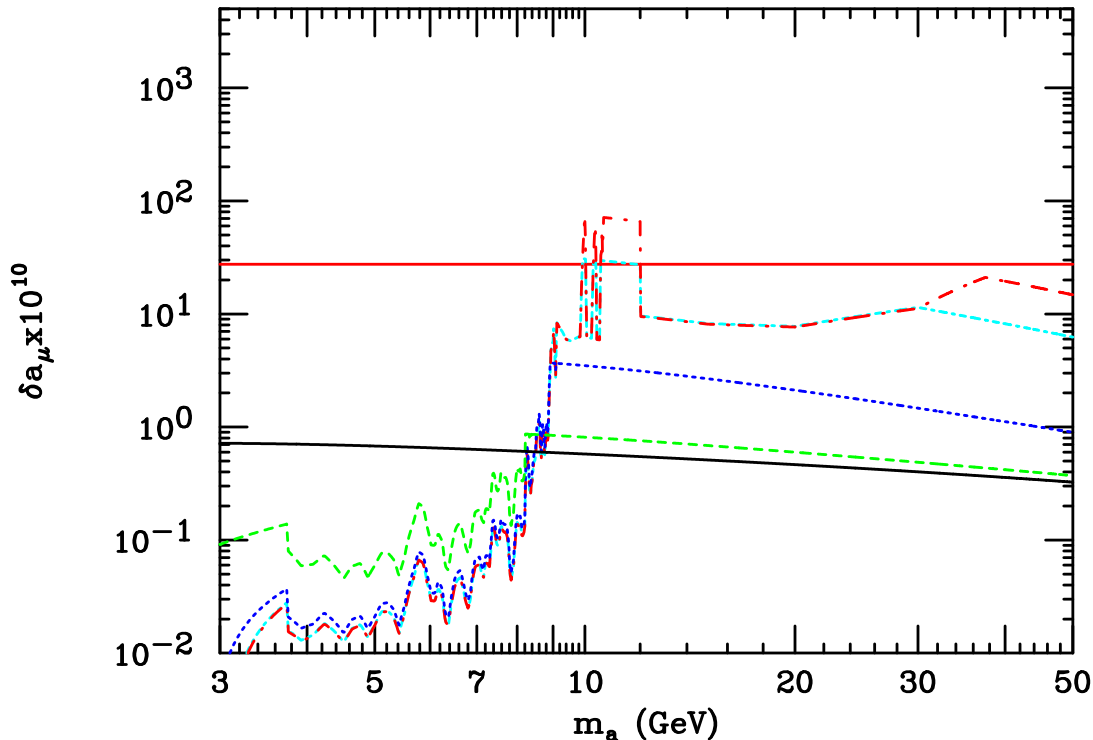


Figure 6: The maximum contribution of the CP-odd a to a_μ as a function of m_a in the NMSSM, for which $C_{abb} = \cos \theta_A \tan \beta$, after employing $\cos \theta_A = \cos \theta_A^{\max}$ where $\cos \theta_A^{\max}$ is plotted for different $\tan \beta$ values in Fig. 5. Curve notation is as in Fig. 5. The horizontal solid red line is located at $\delta a_\mu = 27.5 \times 10^{-10}$.

contributions are multiplied by $(\cos \theta_A)^2$. Thus, when C_{abb}^{\max} is independent of $\tan \beta$ and $\cos \theta_A^{\max} = 1$ (as for $m_a > 12$ GeV and $\tan \beta \lesssim 20$) the resulting δa_μ will always increase with $\tan \beta$. However, at low m_a , the very strong Upsilon constraints on C_{abb} imply that $\cos \theta_A^{\max}$ rapidly decreases with increasing $\tan \beta$ which suppresses the numerically more important 2-loop, top-loop contribution resulting in smaller δa_μ as $\tan \beta$ increases.

From Fig. 6, we observe that the maximal δa_μ can exceed $\Delta a_\mu = 27.5 \times 10^{-10}$ for $9.9 \text{ GeV} \lesssim m_a \lesssim 12 \text{ GeV}$ if $\tan \beta \geq 32$, with an almost precise match to this value of Δa_μ for $\tan \beta = 32$ (or for $\tan \beta$ as low as $\tan \beta = 30$ — see the 2HDM discussion). For $\tan \beta = 50$, one can match Δa_μ by using a value of $\cos \theta_A$ below $\cos \theta_A^{\max}$. (As discussed below, the fact that matching is possible for $9.9 \text{ GeV} \lesssim m_a \lesssim 2m_B$ is particularly interesting in the context of the ideal Higgs scenario.) Further, the maximal δa_μ is in the $7 - 20 \times 10^{-10}$ range for $12 \text{ GeV} < m_a \lesssim 48 \text{ GeV}$ for $\tan \beta = 32$ and for $12 \text{ GeV} < m_a \lesssim 70 \text{ GeV}$ for $\tan \beta = 50$.

At this point, it is worth stressing the other desirable features of the $m_h \sim 100$ GeV, $m_a \lesssim 2m_B$, $BR(h \rightarrow aa) > 0.75$ scenario as discussed in [15, 16, 17, 18]. These references examined the degree to which obtaining the observed value of m_Z requires very precisely tuned values of the GUT scale parameters of the MSSM and NMSSM. One finds that in

any supersymmetric model this finetuning is always minimized for GUT scale parameters that yield a SM-like h with $m_h \leq 100$ GeV, something that is only consistent with LEP data if the h has unexpected decays that reduce the $h \rightarrow b\bar{b}$ branching ratio while not contributing to $h \rightarrow b\bar{b}b\bar{b}$ (also strongly constrained by LEP data). A Higgs sector with a light a for which $BR(h \rightarrow aa) > 0.75$ and with m_a small enough that a decays to $B\bar{B}$ final states are disallowed (i.e. $m_a < 10.56$ GeV) provides a very natural possibility for allowing minimal finetuning. The NMSSM provides one possible example.

In conclusion, the combined limits from Υ decays and $b\bar{b}a$ Yukawa production at LEP, along with the perturbativity requirement of $C_{abb} < 50$, imply that the entire a_μ discrepancy of $\Delta a_\mu \sim 30 \times 10^{-10}$ cannot have a purely Higgs sector explanation without going beyond the MSSM. In the less-constrained NMSSM, achieving $\delta a_\mu \sim \Delta a_\mu$ requires relatively high $\tan\beta$ and a value of m_a between about 10 GeV and $2m_B$. On the one hand, this is a highly motivated m_a region in the NMSSM since, as described earlier, it would allow an “ideal” SM-like h with $m_h \lesssim 100$ GeV decaying mainly via $h \rightarrow aa \rightarrow 4\tau$. Such an h would escape LEP limits while allowing for low m_Z -finetuning. However, on the other hand, in the NMSSM $m_a < 2m_B$ most naturally arises when close to the $U(1)_R$ symmetry limit. In this case, the a is mainly singlet, implying that $\cos\theta_A$ is small and that $C_{abb} = \cos\theta_A \tan\beta$ is typically $\mathcal{O}(1)$ [17], whereas $C_{abb} \sim 30$ is needed to match the observed Δa_μ .

Nonetheless, the possibility that a CP-odd a with 10 GeV $\lesssim m_a \lesssim 12$ GeV could explain the a_μ anomaly should be taken seriously. Thus, finding techniques to experimentally probe for an a in the 10 GeV $< m_a < 12$ GeV region should be a high priority. Such new techniques could either end up limiting C_{abb} sufficiently that Δa_μ cannot be explained in the 2HDM(II) or NMSSM frameworks or else actually allow a discovery of a light a . Of course, this is a region in which $\eta_b - a$ mixing will surely be a complication.

As an aside, one must not forget that in supersymmetric models sparticle loops could have two important roles: (i) they could directly yield large contributions to a_μ ; and (ii) they could modify the relations between $C_{a\mu^- \mu^+}$, $C_{a\tau^- \tau^+}$, C_{abb} and $C_{at\bar{t}}$.

If one goes beyond the MSSM and NMSSM Higgs sectors to the more general type-II 2HDM, then, keeping $C_{abb} < 50$, only an a with 10 GeV $< m_a < 12$ GeV with $C_{abb} \sim 30-32$ could give $\delta a_\mu = \Delta a_\mu$. (A type-I 2HDM gives negative δa_μ that is large for $m_a > 8$ GeV if $C_{abb} = C_{abb}^{\max}$ and is therefore strongly disfavored by the observed positive Δa_μ .)

Obtaining the observed Δa_μ in the most general Higgs model for which the abb coupling magnitude is disconnected from the ratio $R_{b/t}^2$ of the abb to $at\bar{t}$ couplings is generically possible so long as $R_{b/t}^2 > 0$. For $R_{b/t} = 1$, $m_a > 8$ GeV and a relatively modest value of C_{abb} (well below the maximum allowed) will yield $\delta a_\mu = \Delta a_\mu$. As $R_{b/t}$ increases, the required C_{abb} increases. For larger $R_{b/t}$, there are regions of m_a for which the required C_{abb} exceeds the upper experimental bound, C_{abb}^{\max} . Further, $\delta a_\mu = \Delta a_\mu$ cannot be achieved above an $R_{b/t}$ -dependent maximum m_a if $C_{abb} < 50$ is imposed. For $R_{b/t} < 0.2$, even very low values of m_a will yield the observed Δa_μ for an appropriate choice of $C_{abb} < C_{abb}^{\max}$.

Acknowledgments

This work was supported by U.S. DOE grant No. DE-FG03-91ER40674. This research

was supported in part by the National Science Foundation under Grant No. PHY05-51164 while at KITP and by the Aspen Center for Physics. JFG thanks R. Dermisek, T. Han, B. McElrath, and P. Osland for their comments on the manuscript.

References

- [1] D. Chang, W. F. Chang, C. H. Chou and W. Y. Keung, Phys. Rev. D **63**, 091301 (2001) [arXiv:hep-ph/0009292].
- [2] A. Dedes and H. E. Haber, JHEP **0105**, 006 (2001) [arXiv:hep-ph/0102297].
- [3] K. m. Cheung, C. H. Chou and O. C. W. Kong, Phys. Rev. D **64**, 111301 (2001) [arXiv:hep-ph/0103183].
- [4] C. H. W. Chen and C. Q. Geng, Phys. Lett. B **511**, 77 (2001) [arXiv:hep-ph/0104151].
- [5] Y. L. Wu and Y. F. Zhou, Phys. Rev. D **64**, 115018 (2001) [arXiv:hep-ph/0104056].
- [6] M. Krawczyk, arXiv:hep-ph/0103223.
- [7] A. Arhrib and S. Baek, Phys. Rev. D **65**, 075002 (2002) [arXiv:hep-ph/0104225].
- [8] M. Krawczyk, Acta Phys. Polon. B **33**, 2621 (2002) [arXiv:hep-ph/0208076].
- [9] K. Cheung and O. C. W. Kong, Phys. Rev. D **68**, 053003 (2003) [arXiv:hep-ph/0302111].
- [10] O. C. W. Kong, arXiv:hep-ph/0402010.
- [11] F. Domingo and U. Ellwanger, JHEP **0712**, 090 (2007) [arXiv:0710.3714 [hep-ph]].
- [12] F. Domingo and U. Ellwanger, arXiv:0806.0733 [hep-ph].
- [13] M. Davier, Nucl. Phys. Proc. Suppl. **169**, 288 (2007) [arXiv:hep-ph/0701163].
- [14] S. M. Barr and A. Zee, Phys. Rev. Lett. **65**, 21 (1990) [Erratum-ibid. **65**, 2920 (1990)].
- [15] R. Dermisek and J. F. Gunion, Phys. Rev. Lett. **95**, 041801 (2005) [arXiv:hep-ph/0502105].
- [16] R. Dermisek and J. F. Gunion, Phys. Rev. D **73**, 111701 (2006) [arXiv:hep-ph/0510322].
- [17] R. Dermisek and J. F. Gunion, Phys. Rev. D **75**, 075019 (2007) [arXiv:hep-ph/0611142].
- [18] R. Dermisek and J. F. Gunion, Phys. Rev. D **76**, 095006 (2007) [arXiv:0705.4387 [hep-ph]].
- [19] S. Chang, P. J. Fox and N. Weiner, JHEP **0608**, 068 (2006) [arXiv:hep-ph/0511250].
- [20] S. Chang, R. Dermisek, J. F. Gunion and N. Weiner, arXiv:0801.4554 [hep-ph].
- [21] J. Lee-Franzini, Eloisatron Workshop: Higgs 1989:0269-294 (QCD161:I12:1989).
- [22] W. Love, *et al.*(CLEO), CLNS 08/2033, CLEO 08-16 to be submitted to PRL.
- [23] M. Drees and K. i. Hikasa, Phys. Rev. D **41**, 1547 (1990).
- [24] M. A. Sanchis-Lozano, Mod. Phys. Lett. A **17**, 2265 (2002) [arXiv:hep-ph/0206156].
M. A. Sanchis-Lozano, Int. J. Mod. Phys. A **19**, 2183 (2004) [arXiv:hep-ph/0307313].
E. Fullana and M. A. Sanchis-Lozano, Phys. Lett. B **653**, 67 (2007) [arXiv:hep-ph/0702190].
M. A. Sanchis-Lozano, arXiv:0709.3647 [hep-ph].
- [25] G. Abbiendi *et al.* [OPAL Collaboration], Eur. Phys. J. C **23**, 397 (2002) [arXiv:hep-ex/0111010].

- [26] The Delphi Collaboration, ICHEP 2002, DELPHI 2002-037-CONF-571. I employ Table 20 — these are very close to those appearing in the figures of J. Abdallah *et al.* [DELPHI Collaboration], Eur. Phys. J. C **38**, 1 (2004) [arXiv:hep-ex/0410017].
- [27] Nils Krumnack (CDF plus D0 results) talk at ICHEP2008.
- [28] F. Domingo, U. Ellwanger, E. Fullana, C. Hugonie and M. A. Sanchis-Lozano, arXiv:0810.4736 [hep-ph].
- [29] G. Abbiendi *et al.* [OPAL Collaboration], Eur. Phys. J. C **40**, 317 (2005) [arXiv:hep-ex/0408097].
- [30] S. Schael *et al.* [ALEPH Collaboration and DELPHI Collaboration and L3 Collaboration and], Eur. Phys. J. C **47**, 547 (2006) [arXiv:hep-ex/0602042].
- [31] J. R. Ellis, S. Heinemeyer, K. A. Olive, A. M. Weber and G. Weiglein, JHEP **0708**, 083 (2007) [arXiv:0706.0652 [hep-ph]].
- [32] J. R. Ellis, J. F. Gunion, H. E. Haber, L. Roszkowski and F. Zwirner, Phys. Rev. D **39**, 844 (1989).
- [33] U. Ellwanger, J. F. Gunion and C. Hugonie, JHEP **0502**, 066 (2005) [arXiv:hep-ph/0406215].
- [34] U. Ellwanger and C. Hugonie, Comput. Phys. Commun. **175**, 290 (2006) [arXiv:hep-ph/0508022].
- [35] M. S. Chanowitz, arXiv:0806.0890 [hep-ph].